网络出版时间：2014-09-03 10:48
网络出版地址：http://www.cnki.net/kcms/detail/61.1235.O4.20140903.1048.007.html

Fenna-Matthews-Olson 捕光复合物中的冗余结构

冷轩，梁先庭
（宁波大学 理学院 光学研究所，宁波 315211）

摘 要：本文研究了绿色硫细菌中捕光天线复合物Fenna-Matthews-Olson的一个子单元和反应中心的能量传递。首先，通过实验报道的细菌叶绿素分子的能量和它们间的耦合强度，构建了该系统包含反应中心的哈密顿量及约化模型。然后，基于该哈密顿量模型通过级联运动方程研究了不同分子间和反应中心的激子布居演化。最后，为了获得在能量传输过程中不同激子态间的相干性，计算了Fenna-Matthews-Olson及其约化模型的二维三阶光子回波谱。结果显示在能量捕获过程中，Fenna-Matthews-Olson复合物存在冗余结构。该发现将有助于找出一些简化结构来构建人造光合作用材料。

关键词：二维光谱；能量传输；布居演化；相干性；Fenna-Matthews-Olson
中图分类号：O433.4; O413.1 **文献标识码**：A **文章编号**：

Redundancy of Fenna-Matthews-Olson for energy harvesting

LENG Xuan, LIANG Xian-ting
(*Department of Physics and Institute of Optics, Ningbo University, Ningbo* 315211, *China*)

Abstract: The investigated system includes a subunit of Fenna-Matthews-Olson antenna complex of green sulfur bacteria and its reaction center (sink). At first, through fixing the site energies of bacteriochlorophyll molecules and the coupling strength between the BChls, we construct a Hamiltonian of the Fenna-Matthews-Olson-sink and its reduced models. Then, based on the Hamiltonian and by using a hierarchical equation of motion approach we investigate the evolutions of the populations of different BChls and the sink states. Thirdly, in oder to observe the coherence between different states in the processes of energy transfer, we calculate the two-dimensional third-order photon echo spectra of the Fenna-Matthews-Olson and its reduced models in different waiting times. Our results imply that for energy harvesting there may be some redundant chromophores in the Fenna-Matthews-Olson complex. This discovery may be helpful to find out some reduced structures for simulating photosynthesis.

Key words: 2D response laser spectra, Energy transfer, Population evolution, coherence, Fenna-Matthews-Olson
OCIS Codes: 190.4380; 320.7110; 320.7130; 320.7150; 300.6290

0 Introduction

The significance of photosynthesis is indisputable as it is necessary for nearly all life on the Earth. The energies of modern life, for example, oil, coal, natural gas, are all come from photosynthesis. Photosynthesis begins with light harvesting, where the specialized pigment-protein complexes transform sunlight into electronics excitations delivered to reaction center where the energy is used to initiate chemical reactions[1]. Under the pressure of evolution, the light-harvesting systems of plants and bacteria are becoming sophisticated and complex, and the energy transfer efficiency is nearly perfect[2]. The basic mechanism of energy transfer in light harvesting is established by Förster resonance energy transfer (FRET) that the transfer was thought to occur by a classical hopping mechanism[3]. But most surprisingly, the long lived quantum coherence was discovered in light harvesting process, suggested that coherence may play an important role in efficiency energy transport[4]. This discovery thanks to the development of two-dimensional (2D) spectroscopy techniques.

Foundation item: National Natural Science Foundation of China (Grant No. 61078065), the Zhejiang Provincial Natural Science Foundation of China (Grant No. LY13A040006), and the K. C. Wong Magna Foundation in Ningbo University.
First author: Leng Xuan (1989-), male, graduate student, mainly focuses on theoretical simulation of the two dimensional spectroscopy. Email: lengxuan2008@qq.com
Supervisor (Contact author): Liang Xian-ting (1965-), male, professor, Ph.D. degree, mainly focuses on dissipative dynamics of open quantum systems, simulations of multi-dimensional ultrafast laser spectroscopy and quantum information. Email: liangxianting@nbu.edu.cn
Received: Apr. 29, 2014; **Accepted:** Jun. 27, 2014

To date, two-dimensional electronic spectroscopy (2DES) and in particular 2D photon echo (2DPE), is the most common spectroscopy used to explore quantum effects and is considered as the ultimate technique to experimentally detect coherence dynamics[4-6]. Fleming's group in 2005 was first to obtain the 2D spectra of Fenna-Matthews-Olson (FMO) pigment-protein complex which play a role of energy transfer in the green sulfur bacteria[5]. Then, Engel *et al* have reported long-lasting beating signals about 660 fs in 2D spectra of FMO complex at 77 K[4]. After three years, they observed about 300 fs beating signals at physiological temperatures in the same system[6]. The beating signals were interpreted as evidence of quantum coherent energy transfer.

While the experiments developing, a series of theoretical simulations and studies of FMO have been followed. Ishizaki *et al* studied the population evolution of FMO, and pointed out two energy transfer ways[7]. Chen *et al* were first simulated the 2D spectra of FMO by hierarchical equation of motion (HEOM) approach[8]. And the simulations were improved by Hein *et al*[9]. The most interesting is that Nolan *et al* suggested that in terms of energy harvesting, there may be some redundant chromophores in the complex[10]. In general, the photosynthesis systems are very complex. If this kind of redundancy is indeed existed, we may expect to find out some reduced structures for simulating photosynthesis.

In Ref.[10], the master equation of Lindblad operator has been used to investigate the dynamics of FMO. In which, the Lindblad operators are divided into three parts, namely, $\hat{L}_{deph}$, $\hat{L}_{diss}$, and $\hat{L}_{sink}$, which respectively describe the subunit of FMO complex, environment and the sink. In this paper, we shall study the same problem by using another strategy. Here, in the investigating of dynamics, instead of using the Lindblad operators, we take the sink and subunit of the FMO as an entire system and construct a Hamiltonian including them. We suppose that the sink coupled only with the chromophore 3 in one subunit of the FMO[11]. The reduced subsystems also conclude the sink like that. By using the new Hamiltonians and HEOM approach[9,12-17], we investigate the evolutions of populations of the systems. The HEOM approach is an exact numerical method in which some important non-Markovian effects can be included. Considered investigations suggested that the long-lasting quantum coherence of the systems may play significance role for effective energy transfer in photosynthesis systems[4,6,18,19]. Thus, it is interesting that whether the long-lasting coherence still persisted in the reduced structures of the subunit in the FMO in non-markovian environment. We also calculate the 2D third-order laser response spectra based on the HEOM approach. From the 2D response spectra, we observe that there are longer coherent times in not only FMO system but also some of its reduced systems. It means that as for energy transfer the structure of FMO is reducible.

1 Model and Method

The FMO protein of the green sulfur bacterium chlorobium tepidum is a trimer in which each of the three subunits has seven bacteriochlorophyll (BChl) molecules spatially arranged within a distance of several nanometers. As a preliminary study, we treat the three subunits independently. For convenience, the FMO means one of three of the subunits in this paper. The FMO complex plus sink can be described using a Frenkel exciton model. The total Hamiltonian is then written as

$$H = H_{ex} + H_{ph} + H_{ex-ph} \tag{1}$$

Here, H_{ex} describes the exciton system, the motion of the nuclei is modeled by harmonic vibrations $H_{ph} = \sum_{\sigma,m} \hbar\omega_{\sigma,m} b^{\dagger}_{\sigma,m} b_{\sigma,m}$, and H_{ex-ph} is the coupling terms between the exciton and vibrational degrees of freedom. We use the Hamiltonian of the single monomer of the FMO complex is the experimental data that according to Ref. [20]. However, unlike previous studies, here the monomer and reaction center are considered as a complete system, then the system's Hamiltonian can be described as

$$H_{ex} = \sum_{m=1}^{8} \varepsilon_m |m\rangle\langle m| + \sum_{m>n} J_{mn}(|m\rangle\langle n| + |n\rangle\langle m|). \tag{2}$$

The values of the site energies ε_m, and the couplings J_{mn} are listed in Table 1.

Table 1. The Hamiltonian of the single monomer of FMO plus sink.

	BChl1	BChl2	BChl3	BChl4	BChl5	BChl6	BChl7	Sink
BChl1	12400	-106	8	-5	6	-8	-4	0
BChl2	-106	12540	28	6	2	13	1	0
BChl3	8	28	12120	-62	-1	-9	17	-318
BChl4	-5	6	-62	12295	-70	-19	-57	0
BChl5	6	2	-1	-70	12440	40	-2	0
BChl6	-8	13	-9	-19	40	12480	32	0
BChl7	-4	1	17	-57	-2	32	12380	0
Sink	0	0	-318	0	0	0	0	11643

Supposing that the sink is only coupled to the BChl 3 of the FMO because other BChls apart far from reaction center. In Ref.[10], the authors theoretically studied the coupling strength between sink and BChl 3 which is three times large than the largest value of the dipole-dipole coupling between pigments in the FMO complex. We choose the sink energy and its couplings to BChl 3 (in Table 1) according to Ref.[10]. The linear absorption spectrum is given by the Fourier transform of the two-time correlation function of the transition dipole moment (TDM) operator $\boldsymbol{\mu}$ [8,21]:

$$I(\omega) = \mathrm{Re}\int_0^{\infty} e^{i\omega} \langle \boldsymbol{\mu}(t)\boldsymbol{\mu}(0)\rangle_g , \tag{3}$$

where $\boldsymbol{\mu}(t) = e^{iHt/\hbar}\boldsymbol{\mu}e^{-iHt/\hbar}$ is the TDM operator in the Heisenberg picture and $\boldsymbol{\mu} = \sum_m \boldsymbol{\mu}_m(|m\rangle\langle 0| + |0\rangle\langle m|)$ with $\boldsymbol{\mu}_m$ the TDM operator of BChl m. The subscript g indicates that the initial state to calculation the correlation function is equilibrated on the ground electronic state, $\rho_g = |0\rangle\langle 0| \otimes e^{-\beta H_{ph}} / \mathrm{Tr} e^{-\beta H_{ph}}$, where $\beta = 1/K_B T$ with Boltzmann constant K_B and temperature T. The 2D spectra can be obtained from the third order optical response function, which is[9,16]

$$S^{(3)}(\tau_3,\tau_2,\tau_1) = \left(\frac{i}{\hbar}\right)^3 \mathrm{Tr}\{\mu(\tau_3+\tau_2+\tau_1)[\mu(\tau_2+\tau_1),[\mu(\tau_1),[\mu,\rho_g]]]\}. \tag{4}$$

By applying the rotating wave approximation and phase matching, the total response function can be obtained from the rephasing and nonrephasing contributions

$$S^{(3)}(\tau_3,\tau_2,\tau_1) = S_{rp}(\tau_3,\tau_2,\tau_1) + S_{nr}(\tau_3,\tau_2,\tau_1), \tag{5}$$

where,

$$\begin{aligned} S_{rp}(\tau_3,\tau_2,\tau_1) &\equiv \mathrm{Tr}\left\{\mu_- \hat{G}(\tau_3)\mu_+^{\times}\hat{G}(\tau_2)\mu_+^{\times}\hat{G}(\tau_1)\mu_-^{\times}\rho_g\right\}, \\ S_{nr}(\tau_3,\tau_2,\tau_1) &\equiv \mathrm{Tr}\left\{\mu_- \hat{G}(\tau_3)\mu_+^{\times}\hat{G}(\tau_2)\mu_-^{\times}\hat{G}(\tau_1)\mu_+^{\times}\rho_g\right\}. \end{aligned} \tag{6}$$

Here, $G(\tau)$ is the retarded propagator of the total system in the Liouville space. $\tau_1 = t_2 - t_1$, $\tau_2 = t_3 - t_2$, and $\tau_3 = t - t_3$, with t_1, t_2, t_3, the time points of laser projecting to the sample. $\mu_- = \sum \mu_{gm} |g\rangle\langle m|$, $\mu_+ = \sum \mu_{mg} |m\rangle\langle g|$, and $\mu_{\pm}^{\times} A = \mu_{\pm} A - A\mu_{\pm}$. ρ_g is the initial state of the total system,

and we set it in the ground state of the system and in the equilibrium state of the bath initially. In the impulsive limit, the 2D spectra can be described with the double Fourier transforms of S_{nr} and S_{rp} as

$$I(\omega_3,\tau_2,\omega_1)=\mathrm{Re}\int_0^\infty d\tau_1\int_0^\infty d\tau_3\left[e^{i(\omega_1\tau_1+\omega_3\tau_3)}S_{nr}(\tau_3,\tau_2,\tau_1)+e^{i(-\omega_1\tau_1+\omega_3\tau_3)}S_{rp}(\tau_3,\tau_2,\tau_1)\right]. \quad (7)$$

Note, however, that we do not include excited-state absorption (ESA), since our main interest is the detection of coherence survival in this work. ESA is known to influence only the region $\omega_3>\omega_1$ of the 2D profiles; our 2D plots do not reproduce the negative contribution due to ESA in this region [12]. It means that two (two-exciton) pathways in Liouville space have not been included. In order to calculate Eq.(6) with HEOM scheme, we at first calculate $C_1(\tau_1)=\hat{G}(\tau_1)[\mu^{\times}_{-}\rho_g]$ in the process of $\tau_1(t_1\to t_2)$, and then $C_2(\tau_2,\tau_1)=\hat{G}(\tau_2)[\mu^{\times}_{+}C_1(\tau_1)]$ in the process of $\tau_2(t_2\to t_3)$, and then $C_3(\tau_3,\tau_2,\tau_1)=\hat{G}(\tau_3)[\mu^{\times}_{+}C_2(\tau_2,\tau_1)]$. Finally, we calculate $S_{rp}(\tau_3,\tau_2,\tau_1)=\mathrm{Tr}[\mu_{-}C_3(\tau_1,\tau_2,\tau_3)]$. Similarly, we can calculate $S_{nr}(\tau_3,\tau_2,\tau_1)$. In order to perform this calculations, the scheme employed is similar to that used for the calculation of the reduced density matrix $\rho(t)=\mathrm{Tr}_{Bath}[\hat{G}(\tau)\rho(0)]$ with the HEOM. The dynamical approach of the HEOM is a non-Markovian and non-perturbative method[7,8,22,23]. It describes the evolutions of a set of auxiliary density operators $\rho_{\mathbf{n}}$, namely,

$$\begin{aligned}\frac{d}{dt}\rho_{\mathbf{n}}=&-\frac{i}{\hbar}[H_S,\rho_{\mathbf{n}}]-\gamma\sum_{m=1}^{N}n_m\rho_{\mathbf{n}}\\&-\sum_{m=1}^{N}\left[\frac{\eta}{\beta\gamma\hbar^2}-\frac{\eta}{2\hbar}\cot\left(\frac{\beta\gamma\hbar}{2}\right)\right][|m\rangle\langle m|,[|m\rangle\langle m|,\rho_{\mathbf{n}}]]\\&-i\sum_{m=1}^{N}\left[|m\rangle\langle m|,\rho_{\mathbf{n}_m^+}\right]\\&-\frac{i}{\hbar}\sum_{m=1}^{N}n_m\left(c_0|m\rangle\langle m|\rho_{\mathbf{n}_m^-}-c_0^*\rho_{\mathbf{n}_m^-}|m\rangle\langle m|\right),\end{aligned} \quad (8)$$

where

$$c_0=\frac{\eta\gamma}{2}\left[\cot\left(\frac{\beta\gamma\hbar}{2}\right)-i\right]. \quad (9)$$

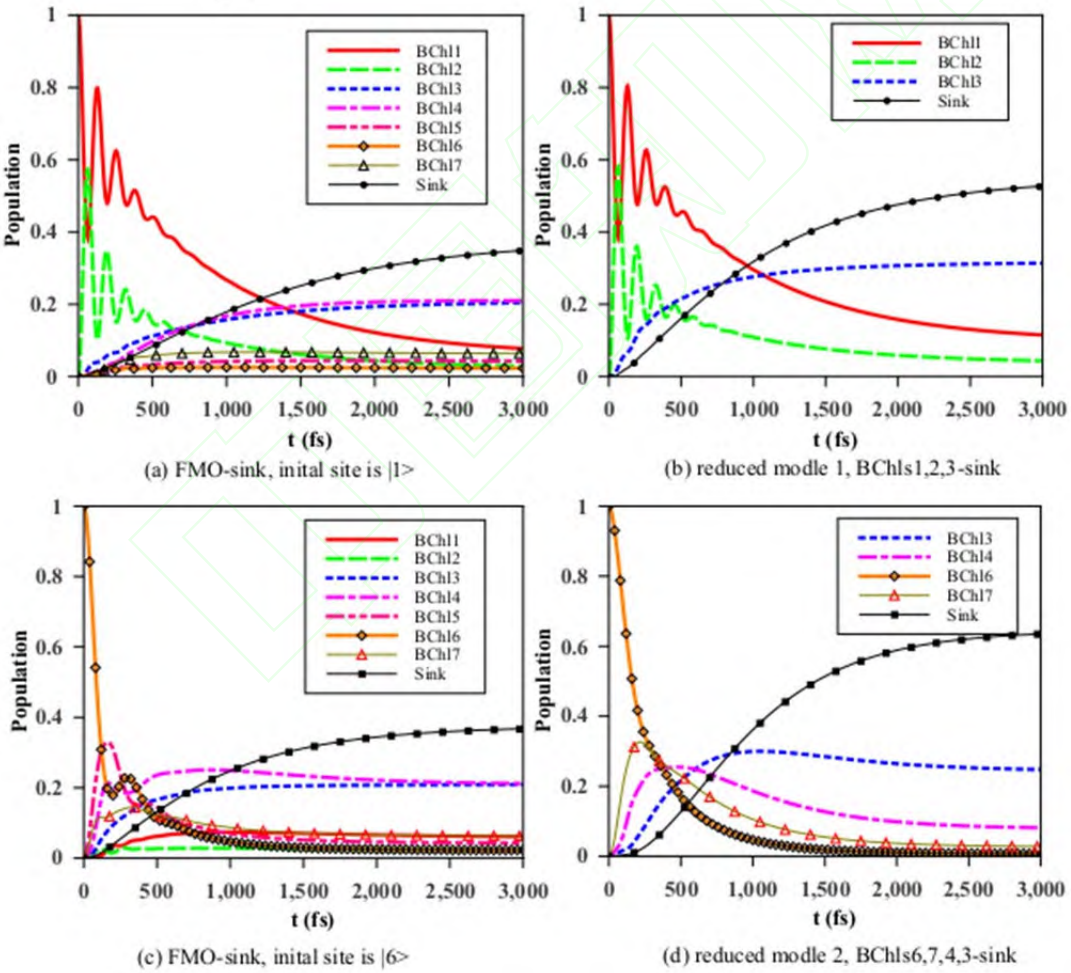

Figure 1. The evolutions of the populations. Here, η = 70 cm^{-1}, T = 77 K, γ^{-1} = 50 fs.

Here, η,γ are parameters of spectral distribution function, where the Drude-Lorentz spectral density function is used, namely we set the spectral density function of the bath be $J(\omega)=\eta\gamma\frac{\omega}{\omega^2+\gamma^2}$, where $\hbar$ denotes the plank constant divided by 2π. The subscript $\mathbf{n}$ denotes the set of index $\mathbf{n}=(n_1,n_2,\cdots,n_n)$, and $\mathbf{n}_m^{\pm}$ differs from $\mathbf{n}$ only by changing the specified $\mathbf{n}_m$. The $\rho_{\mathbf{0}}$ to $\mathbf{n}_m\pm1$ with $\mathbf{0}=(0,0,\cdots,0)$ is the system reduced density operator, while the other $\rho_{\mathbf{n}}s$ are the auxiliary density. Eq. (8) is exact in higher temperature, for example T = 300 K. Here, in order to compare our results with previous work[4,20,24], we set T = 77K, and a

low-temperature correction term is added[7,9,22]. It is shown that at 77 K, Eq. (8) is valid enough[7,9,22].

Here, we consider the disorder of the diagonal terms of the Hamiltonian, and each plot was obtained by averaging over 100 samples with Gaussian distribution and their standard deviations $\sigma = 50cm^{-1}$, whereas off-diagonal disorder was neglected[9,20]. We also consider the rotational average[9], and 100 random directions are used in each plot. The theoretically calculation programs are written by ourselves.

2 Evolutions of populaitons

In order to find out the flow of the excitation energy, in this section we investigate the evolutions of populations of FMO-sink and two reduced FMO-sink models. The values of the Hamiltonians for the two reduced FMO-sink models (model 1 including BChls 1, 2, 3, and model 2 including BChls (6, 7, 4, 3) are listed in Tables 2 and 3, respectively.

Table 2. The Hamiltonian of the reduced FMO(BChl 1,2,3) plus sink.

	BChl1	BChl2	BChl3	Sink
BChl1	12400	-106	8	0
BChl2	-106	12540	28	0
BChl3	8	28	12120	-318
Sink	0	0	-31811643	

For convenience, we set that the photon excitation make the system from ground state $|0\rangle$ to some single excitation state. Here, the single excitation states of BChl 1 to BChl 7 are denoted with $|1\rangle$ to $|7\rangle$. The single excitation state of the sink is denoted with $|8\rangle$. Because there are couplings between different BChls, after some short time the system will populate to different states. The obtained energies of some BChls can be described with the populations of these BChls. We know that a good model for harvesting energy should efficiently transfer energy to the reaction center, the sink. So we are interesting in if the reduced model can keep the same high rate of energy transfer compare to the original one. Therefore, we investigate the FMO-sink and reduced FMO-sink models. The evolutions of the populations of the FMO-sink, and two reduced FMO-sink models are plotted in Fig. 1. Fig. 1(a) and (c) plot the evolutions of states of the FMO-sink model in two different pathways, and the initial states are supposed $|1\rangle$, and $|6\rangle$, respectively. Fig. 1(b) and (d) plot the evolutions of the states of the reduced models 1, and 2 and the initial states are chose as $|1\rangle$ and $|6\rangle$. Here, we set the environmental parameters $\eta = 70$ cm^{-1}, $T = 77$ K, and $\gamma^{-1} = 50$ fs [8,9,10,20].

Table 3. The Hamiltonian of the reduced FMO(BChl 6,7,4,3) plus sink.

	BChl3	BChl4	BChl6	BChl7	Sink
BChl3	12120	-62	-9	17	-186
BChl4	-62	12295	-19	-57	0
BChl6	-9	-19	12480	32	0
BChl7	17	-57	32	12380	0
Sink	-186	0	0	011748	

From Figs. 1(a) and(c) we see that an excitation in BChl 1 will immediately transfer to BChl 3, and BChl 4. After about 2000 fs the transferred energies are mainly concentrated on the sink. Namely, the excitation energies focus on reaction center. Fig. 1(b) and Fig. 1(d) plots the evolutions of the populations of reduced FMO-sink models. From the Fig. 1(b) we see that the evolutions of populations for the states of BChl 1, BChl 2, BChl 3, and sink are the same as them in Fig. 1(a), and the evolutions of populations for the states of BChl 6, BChl 7, BChl 4, BChl 3 and sink from Fig. 1(d) are the same as them in Fig. 1(c) .

These results imply that the reduced FMO models are good enough for transferring energy. It is shown that our results are in agreement with Markovian results reported in Ref.[10]. We have calculated many kinds of subsystem models constructed with different BChls and with different bath parameters and temperature. The results are analogous and the same conclusion can be obtained. The model investigations support a point of view that for energy harvesting the FMO could be reduced, even we consider the non-Markovian effects of the environment. In terms of energy transfer, there are some redundancies in harvesting systems of the photosynthesis.

3 The 2D third-order response spectra

In the following we theoretically investigate the 2D third-order response spectra for the FMO and the reduced FMO models. Here, the sink sites were not included when we calculated the 2D-spectra due to only the purified FMO protein was imaged and thus no sink (reaction center) was attached to the complex in experimental data. The 2D third-order response spectra is an important research tool in probing microstructure and microdynamics[4,5,18,19]. Two reasons motivated our these investigations. At first, the 2D third-order response spectra can more exactly reflect the coherence than the density matrix does. It is more sensitive to the changes of parameters of the system and environment. Secondly, the response spectra can be obtained from the photon echo experiment. The three-pulse photon echo experiment has been developed recent years[4-6,18,19,25-27]. In this kind of experiment, the system to be studied is probed by three incident laser pulses. The first pulse creates an electronic superposition sate between the ground state and the exciton state which evolves for time delay τ_1 until the second pulse interacts with the sample. The second pulse creates a population in the exciton system and the corresponding dynamics is recorded by the population time T. The third pulse interacts with the system to generate a photon echo signal and τ_3 stands for the signal time.

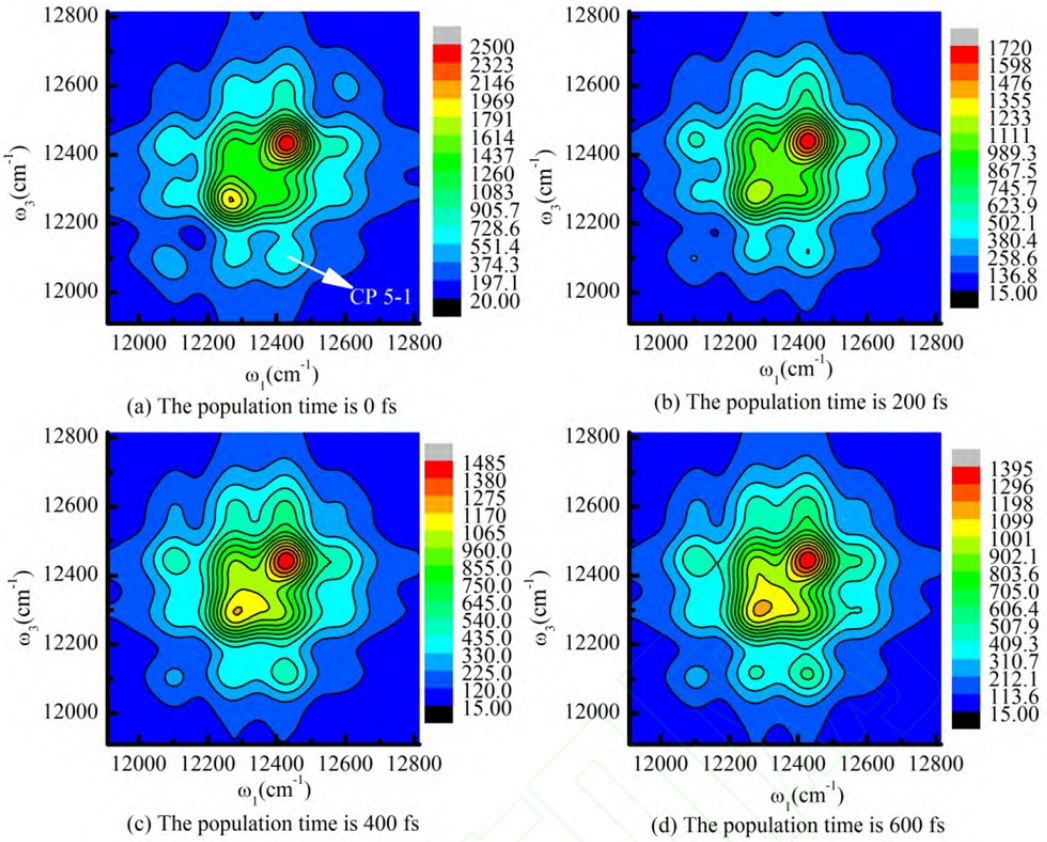

Figure 2. The 2D third order response spectra of full FMO for different population times, where the values of the parameters are the same as them in Fig. 1.

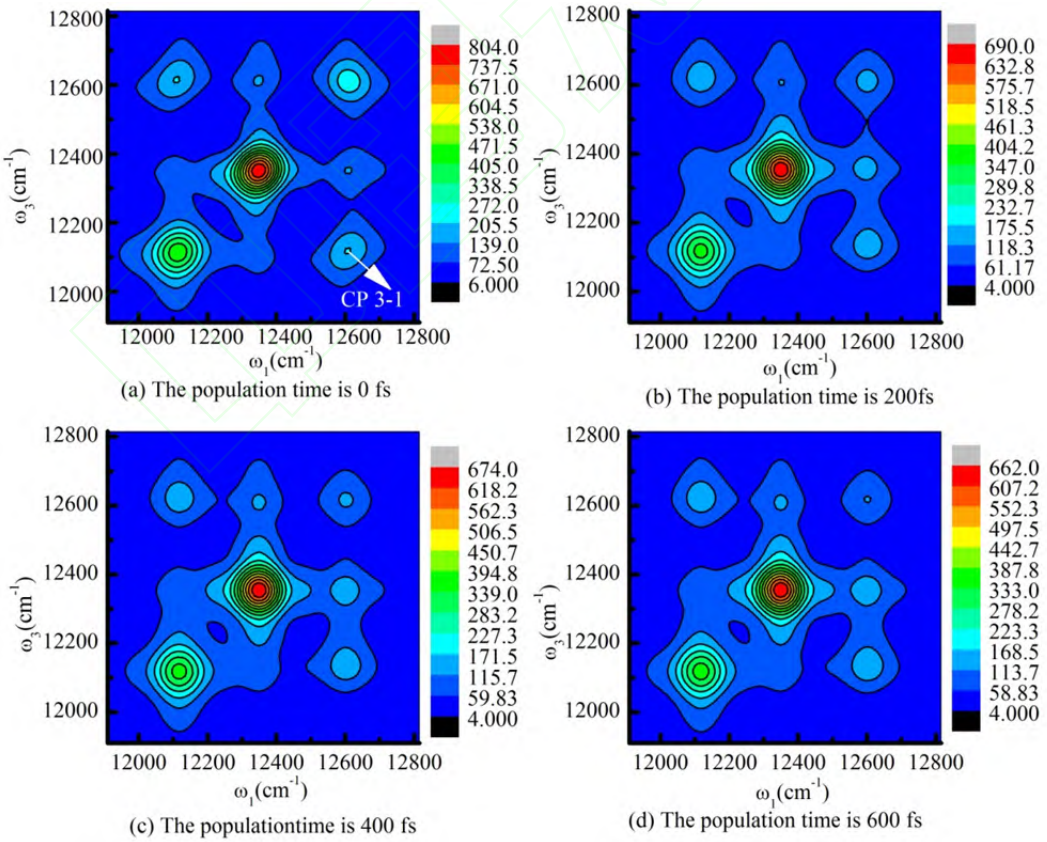

Figure 3. The evolutions of the 2D third-order response spectra of the reduced FMO models 1 , where the values of the parameters are the same as them in Fig. 2.

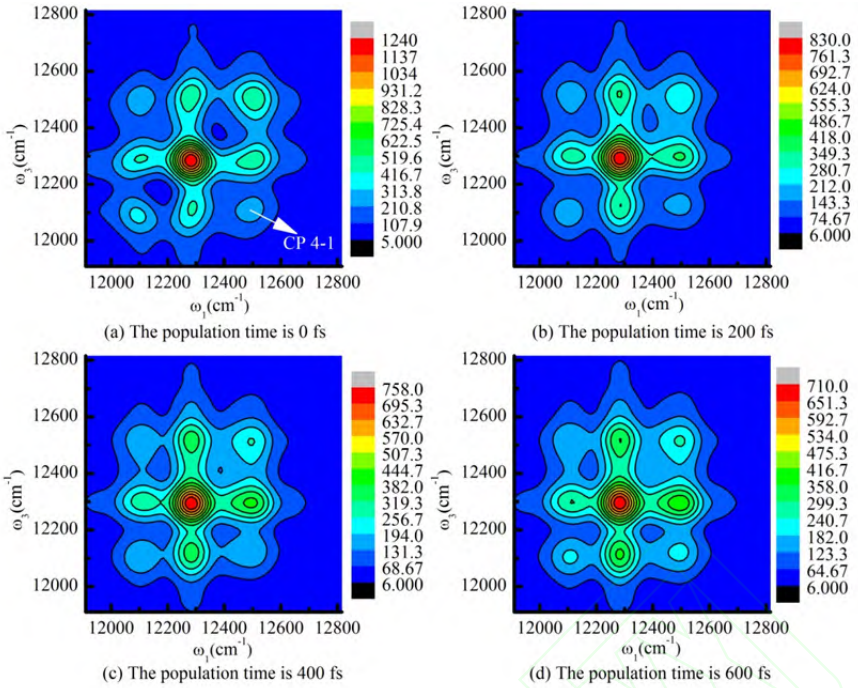

Figure 4. The evolutions of the 2D third-order response spectra of the reduced FMO models 2, where the values of the parameters are the same as them in Fig. 2.

The 2D correlation spectrum obtained from the photon echo experiment can be calculated with Eq. (8). The 2D third-order correlation spectra calculated with the HEOM for the FMO are plotted in Fig. 2. The spectra are in good agreement with the experimental results[8,10]. Here, the spectra with four different population times, namely, T_2 = 0,200,400,600 fs, are plotted. It is shown that the coherence between $|3\rangle$ and other states described with off-diagonal peaks of the left column and the last row become more stronger within 600 fs as the population times increase. The BChl 3 is coupled with the reaction center (sink), and it has stronger coherence with the sink state. So, due to damping of the environment, there are more and more populations collapse to the sink state. The 2D correlation spectra calculated with HEOM for the reduced FMO, constructed with BChls 1, 2 , 3, and sink are plotted in Fig. 3. Here the population times are the same as them in Fig. 2. The results are similar to Fig. 2. Namely, the coherence between the state $|3\rangle$ and other states become more and more strong, and there are more and more populations on the state $|3\rangle$ within 600 fs. The BChl3 is coupled with the sink, so finally, the excitation of BChl1 can be transferred to sink effectively. From the evolutions of the correlation spectra of the FMO and the reduced FMO we can obtain that the excitation energy can be effectively transferred to reaction center in these models. However, the 2D spectra experiments of reduced model have not been done. We hope our reduced model theoretical results can be compared with the future experimental ones.

Table 4. Exciton energy levels(cm^{-1}) of FMO and reduced models.

Exciton	1	2	3	4	5	6	7
FMO	12096	12259	12344	12396	12431	12528	12600
Reduced model 1	12117	12345	12598				
Reduced model 2	12100	12280	12400	12496			

In Fig. 5, we plot the oscillations of cross peaks for 2D-spectra. The cross peaks are the evidence of coherence of the light-harvesting systems. The exciton energy levels of FMO and its reduced models are listed in Table 4. It is shown that the cross peak (CP i-j) oscillations with a frequency corresponding to the difference of its exciton energy $E_i - E_j$ [9,18,24]. Theoretically, the cross peak CP 5-1 of FMO, CP 3-1 of reduced model 1, and CP 4-1 of model 2 should be with the periods of 99.5 fs, 69.3fs and 84.2 fs, respectively. From Fig. 4, we can see that the theoretical periods are good agreement with numerical results. In FMO and reduced FMO models the coherence can persist almost the same time. These results demonstrate that the reduced structure of light harvesting could maintain the long-lasting coherence as the original one.

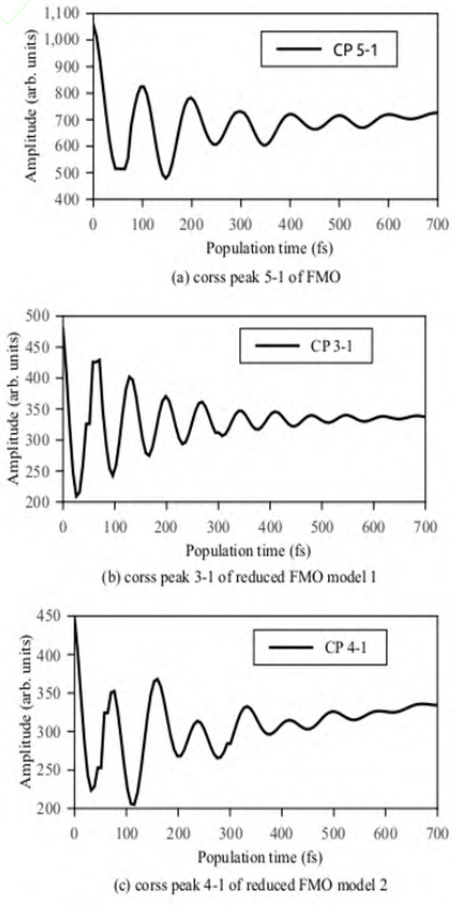

Figure 5. The oscillations of 2D spectra cross peaks with population time.

4 Conclusion

In this paper, we investigate the evolutions of the populations for FMO-sink and its two reduced models. We constructed the model Hamiltonian for the systems, applied a recently developed exact numerical simulation approach, HEOM method, and investigated the evolutions of the dynamics and the 2D third-order response spectra. It is shown that the FMO-sink as well as its reduced models can effectively transfer the energy to the sink, namely, the reaction center. From the 2D correlation spectra we deduce that the efficient energy transfer of the models are resulting from the coupling of sate $|3\rangle$ of BChl 3 with the sink state of the reaction center. And the coherence of the reduced models can persist as long as the FMO does.

In T = 77 K, our investigations are agreement with the Markovian results that discovered in Ref [10]. Namely, there are some redundant chromophores in the complex, which means that it may be possible to find out some reduced structures for simulating photosynthesis.

References

[1] Cheng Yuan-chun, FLEMING R. Dynamics of light harvesting in photosynthesis[J]. *Annual review of physical chemistry*, 2009, **60**(241): 241-62.

[2] SENSION R. Quantum path to photosynthesis[J]. *Natur*e, 2007, **446**(12) : 740.

[3] JANG S, NEWTON M, SILBEY J. Multichromophoric förster resonance energy transfer from B800 to B850 in the light harvesting complex2: evidence for subtle energetic optimization by purple bacteria[J]. *The Journal of Physical Chemistry B*, 2007, **111**(24): 6807-6814.

[4] ENGEL S, CALHOUN R, READ L, *et al*. Evidence for wavelike energy transfer through quantum coherence in photosynthetic systems[J]. *Nature*, 2007,**446** (7137): 782-786.

[5] BRIXNER T, STENGER J, VASWAN M, *et al*. Two-dimensional spectroscopy of electronic couplings in photosynthesis[J]. *Nature*, 2005, **434** (7033): 625-628.

[6] PANITCHAYANGKOON G, HAYES D, FRANSTED K, *et al*. Long-lived quantum coherence in photosynthetic complexes at physiological temperature[J]. *Proceedings of the National Academy of Sciences*, 2010, **107**(29): 12766-12770.

[7] ISHIZAKI A, FLEMING R. Theoretical examination of quantum coherence in a photosynthetic system at physiological temperature[J]. *Proceedings of the National Academy of Sciences* 2009, **106** (41): 17255-17260.

[8] Chen Li-ping, Zheng Ren-hui, Yan Yi-jing, Shi Qiang. Simulation of the two-dimensional electronic spectra of the Fenna-Matthews-Olson complex using the hierarchical equations of motion method[J]. *The Journal of Chemical Physics*,2011, **134** (19): 194508.

[9] HEIN B, KREISBECK C, KRAMER T, *et al.* Modelling of oscillations in two-dimensional echo-spectra of the Fenna-Matthews-Olson complex[J]. *New Journal of Physics*, 2012, **14** (2): 023018.

[10] SKOCHDOPOLE N, MAZZIOTTI A. Functional Subsystems and Quantum Redundancy in Photosynthetic Light Harvesting[J]. *The Journal of Physical Chemistry Letters*, 2011, **2** (23): 2989-2993.

[11] ALICKI R, MIKLASZEWSKI W. A resonance mechanism of efficient energy transfer mediated by Fenna-Matthews-Olson complex. *The Journal of Chemical Physics*, 2012, **136** (13): 134103.

[12] SHARP Z, EGOROVA D, DOMCKE W. Efficient and accurate simulations of two-dimensional electronic photon-echo signals: Illustration for a simple model of the Fenna-Matthews-Olson complex[J]. *The Journal of Chemical Physics*, 2010, **132** (1): 014501.

[13] TANIMURA Y, KUBO R. Time evolution of a quantum system in contact with a nearly Gaussian-Markoffian noise bath[J]. *J. Phys. Soc. Jpn*, 1989, **58** (1): 101-114.

[14] ISHIZAKI A, TANIMURA Y. Quantum dynamics of system strongly coupled to low-temperature colored noise bath: reduced hierarchy equations approach[J]. *Journal Physical Society of Japan*, 2005, **74**(12): 3131.

[15] ISHIZAKI A., TANIMURA Y. Nonperturbative non-Markovian quantum master equation: Validity and limitation to calculate nonlinear response functions[J]. *Chemical Physics*, 2008, **347** (1): 185-193.

[16] CHEN Li-ping, Zheng Ren-hui, Shi Qiang, *et al*. Two-dimensional electronic spectra from the hierarchical equations of motion method: Application to model dimmers[J]. *The Journal of Chemical Physics*, 2010, **132** (2): 024505.

[17] STRUMPFER J, SCHULTEN K. Open quantum dynamics calculations with the hierarchy equations of motion on parallel computers[J]. *Journal of Chemical Theory and Computation*, 2012, **8** (8): 2808-2816.

[18] COLLINI E, WONG C, WILK E, *et al*. Coherently wired light-harvesting in photosynthetic marine algae at ambient temperature. *Nature*, 2010, **463** (7281): 644-647.

[19] WONG Y, ALVEY M, TURNER B, *et al*. Electronic coherence lineshapes reveal hidden excitonic correlations in photosynthetic light harvesting. *Nature Chemistry*, 2012, **4** (5): 396-404.

[20] CHO M, VASWANI M, BRIXNER T, *et al*. Exciton analysis in 2D electronic spectroscopy[J]. *The Journal of Physical Chemistry B*, 2005, **109** (21): 10542-10556.

[21] SCHIJVEN P, MUEHLBACHER L, MUELKEN O. Energy transfer properties and absorption spectra of the FMO complex: from exact PIMC calculations to TCL master equations[J]. *ArXiv e-prints* 2013, (Jan.).

[22] STRUMPFER J, SCHULTEN K. Open Quantum Dynamics Calculations with the Hierarchy Equations of Motion on Parallel Computers. *Journal of Chemical Theory and Computation* **2012**, *8* (8), 2808-2816.

[23] ZHANG Pan-pan, Liu Zhi-qiang, Liang Xian-ting. Two-dimensional electronic spectra investigated using hierarchical equation of motion and cumulant expansion[J]. *Journal of Modern Optics*, 2013, **60** (4): 301-308.

[24] SHARP Z, EGOROVA D, DOMCKE W. Efficient and accurate simulations of two-dimensional electronic photon-echo signals: Illustration for a simple model of the Fenna-Matthews-Olson complex. *The Journal of Chemical Physics* **2010**, *132* (1), 014501.

[25] CARAM R, ZHENG H, DAHLBERG D, *et al*. Persistent interexcitonic quantum coherence in CdSe quantum dots[J]. *The Journal of Physical Chemistry Letter*s, 2013, **5** (1): 196-204.

[26] DAHLBERG D, FIDLER F, CARAM R, *et al*. Energy transfer observed in live cells using two-dimensional electronic spectroscopy[J]. *The Journal of Physical Chemistry Letters*, 2013, **4** (21): 3636-3640.

[27] FIDLER F, SINGH P, LONG D, *et al*. Probing energy transfer events in the light harvesting complex 2 (LH2) of Rhodobacter sphaeroides with two-dimensional spectroscopy. *The Journal of Chemical Physics*, 2013, **139** (15):155-101